Journal of Fluorescence, Vol. 14, No. 1, January 2004 (©2004)

Pseudo Real-Time Method for Monitoring of the Limiting Anisotropy in Membranes

P. Herman,[1,3] J. Malinsky,[2] J. Plasek,[1] and J. Vecer[1]

Received August 31, 2003; revised October 20, 2003; accepted October 20, 2003

Data acquisition and analysis of the time-resolved fluorescence anisotropy is typically a time consuming process preventing usage of this experimental method for monitoring of time-dependent phenomena. We describe a method for pseudo real-time monitoring of the limiting fluorescence anisotropy r_∞ allowing to track changes of the membrane order occurring on the time scale of minutes. Principle and performance of the method is demonstrated in the time domain with the time-correlated single photon counting detection. DMPC liposomes stained with 1,6-diphenyl-1,3,5-hexatriene (DPH) have been used to test influence of the diffusion membrane potential on the membrane order during the temperature-induced phase transition in DMPC membranes. It has been found that the transmembrane field of the order of -70 mV increases the phase transition temperature by about 1.5°C–2°C. It is proposed that the full advantage of the method can be utilized with a gated detection, which besides a faster data acquisition brings additional advantage of excitation light suppression. The method can be also used for imaging.

KEY WORDS: Fluorescence anisotropy; limiting anisotropy; gating; membrane potential; DPH; phase transition; DMPC; LUV.

INTRODUCTION

Understanding of biological functions of lipid membranes requires knowledge of their structure and physical characteristics. Time-resolved polarized fluorescence techniques and hydrophobic fluorescence probes introduced to the lipid membrane offer a great possibility for studying rotational diffusion of the probes. Since the reorientation of the fluorophore reflects its interactions with lipid chains, the fluorescence anisotropy reports on their statistical order and dynamics [1]. When the probe resides in an anisotropic environment where its motion is angularly restricted, e.g. membrane, the time resolved fluorescence anisotropy $r(t)$ does not decay to zero [2,3]. Number of groups experimentally demonstrated that $r(t)$ reaches certain limiting value r_∞ in membranes [4–7]. Kinosita *et al.* was the first who theoretically related characteristics of the fluorescence anisotropy to membrane properties by introduction of the wobble-in-cone model [3]. Later theoretical analyses have shown that r_∞ is directly related to the second-rank order parameter $\langle P_2 \rangle$ by the relation $r_\infty = r_0 \langle P_2 \rangle^2$ [8–12], where r_0 is an initial fluorescence anisotropy. The r_0 is experimentally measurable and is characteristic for the probe used only. From this point of view r_∞ and $\langle P_2 \rangle$ carry the same information.

Measurement of the time resolved fluorescence data by standard time domain [13] or frequency domain [14,15] methods is a time consuming process typically requiring minutes, sometimes even hours, of the data acquisition time. Additional time is needed for the data analysis [13,16]. This prevents usage of the methods for monitoring of dynamic processes. Attempts have been done to develop devices capable of fast data acquisition by massively parallel data collection, the effort, however, resulted in a rather complex and expensive devices [17,18].

[1] Institute of Physics, Charles University, Ke Karlovu 5, 121 16 Prague 2, Czech Republic.
[2] Institute of Experimental Medicine, Academy of Sciences of Czech Republic, Prague, Czech Republic.
[3] To whom correspondence should be addressed. E-mail: herman@karlov.mff.cuni.cz

1053-0509/04/0100-0079/0 © 2004 Plenum Publishing Corporation

We have developed a simple method allowing assessment of r_∞ in seconds by reducing the information extracted from the anisotropy decays and by complete elimination of the time-consuming reconvolution data analysis. The method is fast enough to measure slow processes on the time scale of minutes.

Number of physical factors can modulate physical properties of the biological membranes. One of them is a membrane potential, which is essential for living cell. An important component of the transmembrane electric field is the diffusion potential ψ created by ion gradients across the membrane. Understanding how the strong transmembrane field modulates the structural organization of the lipid bilayer itself is of great interest since a barrier function of the bilayer under wide range of external conditions is critical for all living cells. This was the motivation to apply the method for detection of potential-driven structural changes in synthetic lipid bilayer during the phase transition.

THEORY

Prior to demonstration of the direct r_∞ measurement we will describe the theory and principles of the method. Intuitive description of the r_∞ measurement is presented in Fig. 1. The anisotropy decay is described by the formula:

$$r(t) = \frac{I_\parallel(t) - I_\perp(t)}{I_\parallel(t) + 2I_\perp(t)} = \frac{I_\parallel(t) - I_\perp(t)}{I(t)} \qquad (1)$$

where $I(t)$ is a fluorescence intensity decay and $I_\parallel(t)$ and $I_\perp(t)$ are fluorescence components polarized parallel and perpendicularly to the polarization of the excitation pulse. Suppose that the fluorescence probe is placed in the environment restricting its angular reorientation. Under such circumstances the anisotropy does not decay to zero reaching limiting value r_∞. The anisotropy decay is complex in most cases, however, for simplicity we can assume a monoexponential decay [3]:

$$r(t) = (r_0 - r_\infty) \cdot e^{-t/\phi} + r_\infty \qquad (2)$$

where the r_0 and ϕ are the initial anisotropy and the rotational correlation time, respectively. From Fig. 1C and Eq. (2) it is seen that after time t_1 the time-dependent terms of the anisotropy decay die off. For instance after time $t_1 = 4\phi$ the exponential term of the fluorescence anisotropy decays below 2% of its original value and the anisotropy remains with reasonable accuracy constant. If we were able to measure $r(t)$ at any time $t > t_1$, we would obtain value $r(t) = r_\infty$. In order to increase signal to noise (S/N) ratio it is advisable to collect as many photons as possible and integrate decays $I_\parallel(t)$ and $I_\perp(t)$ over the time interval $\langle t_1, t_2 \rangle$, Fig 1B:

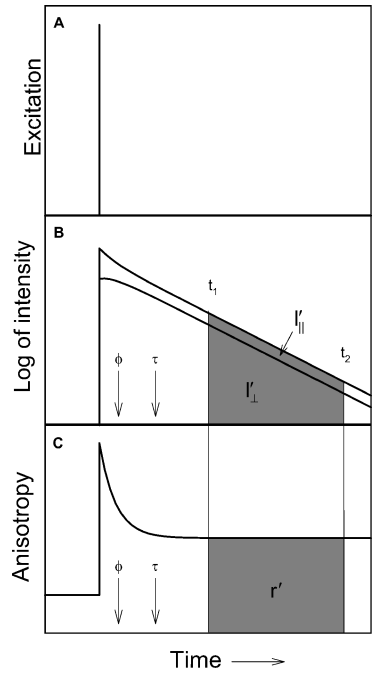

Fig. 1. Intuitive description of the limiting anisotropy measurements. (A) Pulse excitation, (B) polarized fluorescence decays, (C) fluorescence anisotropy decay. The parameter values used for the simulations are $\tau =$ 10 ns, $\phi = 3$ ns, $r_0 = 0.4$, $r_\infty = 0.15$. The collection of the polarized components $I'_\parallel$ and $I'_\perp$ started at $t_1 = 20$ ns and finished at $t_2 = 45$ ns after the excitation pulse.

$$I'_\parallel = \int_{t_1}^{t_2} I_\parallel(t)\,dt, \quad I'_\perp = \int_{t_1}^{t_2} I_\perp(t)\,dt \qquad (3)$$

The upper integration limit t_2 can be set to any value $t_2 > t_1$. The larger is the value of t_2 the more photons from the decay is collected and S/N ratio improves. However, increasing of t_2 to values larger then about five fluorescence lifetimes, $t_2 > 5\tau$, does not bring further significant improvement of the S/N ratio, since the intensity $I(t)$ has already decayed below 0.7% of its original value and almost no photons left to collect. Even more, collection of background and noise signal in the region of very weak emission could eventually bias the measurement and should be avoided. An optimal value of t_2 has to be chosen according to the instrument sensitivity and noise.

The anisotropy r' calculated from the integral intensities $I'_\parallel$ and $I'_\perp$ is given by formula:

$$r' = \frac{I'_\parallel - I'_\perp}{I'_\parallel + 2I'_\perp} = \frac{\int_{t_1}^{t_2} I(t) \cdot r(t)\,dt}{\int_{t_1}^{t_2} I(t)\,dt} \qquad (4)$$

By substituting Eq. (2) and for $t_1 \gg \phi$ we obtain:

$$r' = \frac{I'_{\parallel} - I'_{\perp}}{I'_{\parallel} + 2I'_{\perp}} = \frac{\int_{t_1}^{t_2} I(t) \cdot (r_0 - r_\infty) \cdot e^{-t/\phi}\, dt}{\int_{t_1}^{t_2} I(t)\, dt} + r_\infty \approx r_\infty \quad (5)$$

It should be stressed that Eq. (5) holds true for any $r(t)$ decaying to the limiting value r_∞. For assessment of the r_∞ from Eq. (5) is not necessary to know the exact shape of the anisotropy decay, assuming that the starting integration limit t_1 is large enough compared to the longest rotation correlation time in the decay. Since only integral signals $I'_{\parallel}$ and $I'_{\perp}$ are collected, the anisotropy r' can be instantaneously calculated according to Eq. (5) without need of a complicated deconvolution analysis. Measurements with such setup resemble standard steady state anisotropy experiment.

It is instructive to inspect to which extent the light sensitivity of the instrument is affected by discarding the early parts of the fluorescence decays. When assuming a monoexponential decay and the lower integration limit set to $t_1 = 4\phi$, the measured fraction F of the fluorescence intensity is:

$$F = \frac{\int_{4\phi}^{\infty} I_0 \cdot e^{-t/\tau}\, dt}{\int_0^{\infty} I_0 \cdot e^{-t/\tau}\, dt} = e^{-4\phi/\tau} \quad (6)$$

From Eq. (6) it is seen that the method cannot be used for samples where $\phi \approx \tau$, since no emission remains after $r(t)$ reaches the plateau. The light collection efficiency rapidly increases with decreasing ratio of ϕ/τ. For values used in simulation in Fig. 1, i.e. $\tau = 10$ ns and $\phi = 3$ ns, we obtain $F = \exp(-12/10) = 0.3$. Fortunatelly, the ratio F for the favorite membrane probe DPH is usually close to the number given in the example and the experiment can be accomplished. Employment of long-lived fluorophores such as metal-ligand complexes (MLC) [19–23] with microsecond lifetimes [24] would bring the F ratio close to 100%.

It is easy to envision that the described method can be easily accomplished with a gated detection. The detector, which is normally gated off, is gated on and off at the time t_1 and t_2 after excitation, respectively. Cutoff ratios larger than 7×10^5 have been reported for side window PMTs [25], so we believe that a complete suppression of signal outside the time window $\langle t_1, t_2 \rangle$ can be readily accomplished. An additional advantage of the gating approach is an effective suppression of the scattered excitation light which is known to severely affect measured anisotropy values [25–27].

MATERIALS AND METHODS

Measurement of r_∞

In this report we have used an alternative approach to the gating. We have employed time-correlated single photon counting (TCSPC) for direct measurement of r_∞. The block diagram of the instrument is shown in Fig. 2. Picosecond excitation at 355 nm with a 4 MHz repetition rate obtained after doubling the 710 nm output of the cavity-dumped dye laser (Spectra Physics) with the Pyridine 1 dye. Emission was accumulated at 430 nm. The wavelength was selected by monochromator with the slit-width of 8 nm. A glass absorption filter with the cut-off wavelength of 400 nm was placed in front of the input slit for better rejection of the scattered light. The polarized signals were measured with the emission polarizer set in the fixed vertical position and the excitation polarization plane was rotated between 0 deg and 90 deg, respectively, by the PC-controlled quartz polarization-rotator. This approach minimized the correction for unequal transmittances of

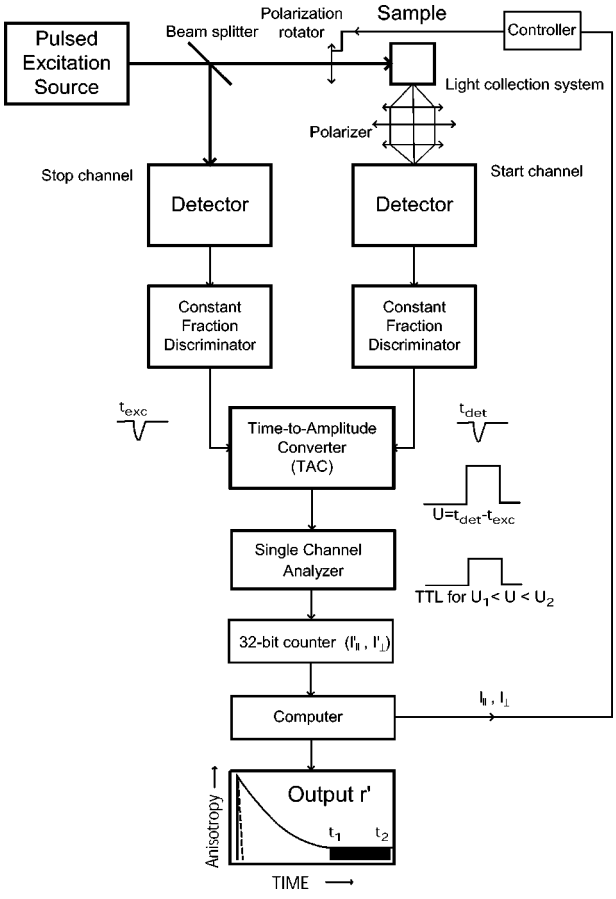

Fig. 2. Block diagram of the apparatus.

the detection channel for different polarizations, since the G-factor was close to one. This was verified by an independent experiment.

We have used NIM modules from EG&G Ortec as components of the TCSPC detection. Output from the time-to-amplitude converter was analyzed by a single channel analyzer (SCA), Ortec 567, which is generating a TTL pulse for any fluorescence photon detected at the time window $\langle t_1, t_2 \rangle$. Photons outside the interval are rejected. The limits t_1 and t_2 are freely adjustable. Number of the pulses, equal to the integral intensity in the time window $\langle t_1, t_2 \rangle$, was counted by a plug-in card CTM05 (Metra Byte) configured as a fast 32-bit counter. The polarized intensities $I'_{\parallel}$ and $I'_{\perp}$ were sequentially measured, stored in the computer memory, and the anisotropy r' was immediately calculated. Values of r_∞ can be obtained every 5–20 s which is much faster then the classical approach and not much worse then the time typically required for acquisition of the steady state fluorescence anisotropy.

Fluorescence and Anisotropy Decays

Full fluorescence and anisotropy decays were acquired with the standard TCSPC setup. The apparatus response function was reconstructed from emission of a pair of reference compounds [28]. The time resolved data were fitted by the standard least squares method. The general model [16,29] has been used for fitting the fluorescence anisotropy decays [30].

Samples were measured in a thermostatic holder connected to the programmable water bath. Temperature was measured directly in the cuvette by thermocouple with an accuracy of 0.1°C. For the temperature scans the temperature measurements were synchronized with the data collection and readings were stored in the PC.

Chemicals and Buffers

*D*imyristoylphosphatidylcholine (DMPC) was purchased from Sigma, 1,6-dipheny-1,3,5-hexatriene (DPH) was obtained from SERVA, and diS-C_3(3) from Molecular Probes. Other chemicals, all analytical grades, were obtained from FLUKA.

The TK and TC buffers were prepared by supplying the 17 mM Tris-base solution by 150 mM KCl and 150 mM choline chloride, respectively. The pH of the both buffers was adjusted to 7.4 by the hydrochloric acid.

Liposome Preparation

Lipid dissolved in chloroform was dried on the test tube wall under nitrogen and kept in a vacuum for at least 15 min. Large multilamellar vesicles (MLV), 25 mM total DMPC concentration, were formed by hand-shaking of the dried lipid film with the TK buffer. Large unilamellar liposomes (LUVs) were extruded by 21 passages of the MLV suspension through the polycarbonate filter, 0.4 μm pore diameter (Nuclepore Corp., Pleasanton, CA) [31]. The extrusion was done above the phase transition temperature, at 40°C.

The diffusion membrane potential was set by procedure of Vecer *et al.* [32]. The potential was created by the K^+ ion gradient on the liposomal membrane. Liposomes prepared in the TK buffer and containing 150 mM K^+ inside were diluted 250× (v/v) by the TC buffer contaning 150 mM choline chloride instead of KCl. The value of the transmembrane potential generated by this method was estimated to be about −70 mV, negative inside [32]. The presence of the membrane potential was verified with the potentiometric indicator diS-C_3(3) [32–34]. Liposomes without the membrane potential were prepared by diluting the stock LUV suspension by the TK buffer to the final concentration of 100 μM lipid/mL. Diluted samples were stained by DPH, 5×10^{-7} M final probe concentration. The sample preparation was done at 40°C and the resulting LUV suspension was kept well above the DMPC phase transition temperature until measured.

RESULTS

The direct measurement of r_∞ is demonstrated on the phase transition in the model DMPC membrane monitored by fluorescence of DPH. We have tested influence of the diffusion membrane potential on the lipid order during the main phase transition. Before describing the experiment we will examine validity of the approach under our particular conditions. In order to set the time window on the SCA, we have measured full fluorescence anisotropy decays at the low and high ends of the temperature range used, Figs. 3 and 4. Figures 3A and 4A show polarized fluorescence decays of DPH in the DMPC vesicles at 15°C and 30°C, respectively. Consistently with literature [16], the least squares data analysis revealed a biexponential fluorescence decay of DPH with the mean lifetime close to 10.6 ns and 8.8 ns at 15°C and 30°C, respectively. The parallel decays of $I_{\parallel}(t)$ and $I_{\perp}(t)$ at long times after the excitation indicate incomplete fluorescence depolarization and a significant value of r_∞, Fig. 3A. Inspection of the anisotropy decay at 15°C, Fig. 3B, reveals that $r(t)$ rapidly decays to the limiting value of $r_\infty = 0.33$ and within the experimental accuracy stays constant. This is true from about 10 ns to 50 ns after excitation when DPH fluorescence diminishes. At 15°C the DMPC membrane is in the

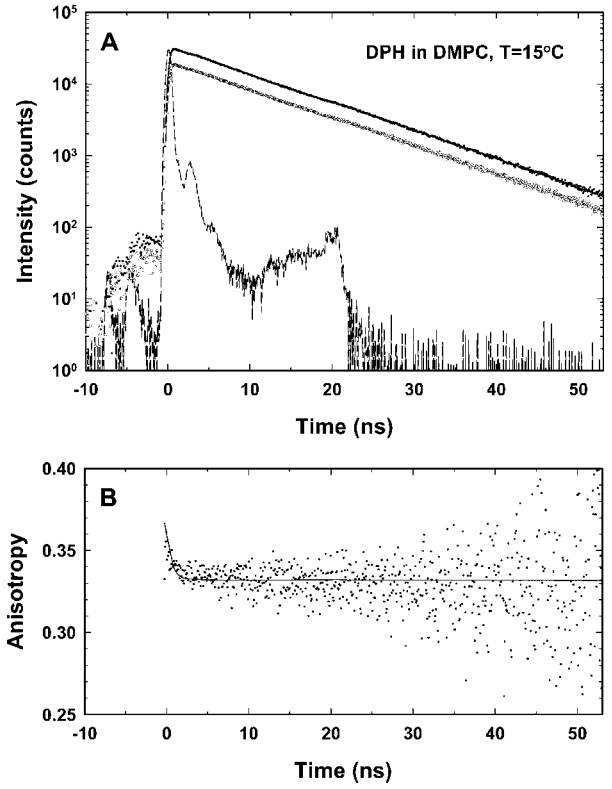

Fig. 3. Fluorescence decay (A) and anisotropy decay (B) of DPH-stained DMPC liposomes at 15°C. The dashed line in the panel (A) is an apparatus response function. Solid lines indicate the best least squares reconvolution fit of the data. The solid line in the panel (B) is an anisotropy calculated from the fitted curves.

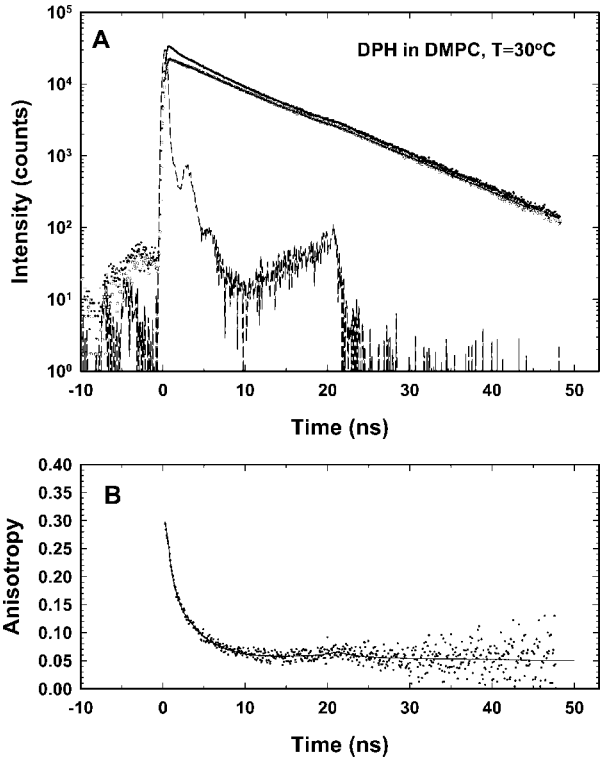

Fig. 4. Fluorescence decay (A) and anisotropy decay (B) of DPH-stained DMPC liposomes at 30°C. The dashed line in the panel (A) is an apparatus response function. Solid lines indicate the best least squares reconvolution fit of the data. The solid line in the panel (B) is an anisotropy calculated from the fitted curves.

gel phase and the high r_∞ value reflects high lipid order below the phase-transition temperature.

Figure 4B displays anisotropy decay of DPH at 30°C, i.e. above the phase transition temperature of DMPC membranes. It is seen that in the liquid phase the $r(t)$ decays to much lower limiting value of $r_\infty = 0.051$ reflecting higher rotational freedom of DPH and higher disorder of the lipid bilayer. Small increase of the anisotropy located near 20 ns correlates with the afterpulse in the apparatus response function. Such afterpulse is typical for conventional head-on PMTs and prevents setting of the t_1 limit closer then about 25 ns after the excitation pulse. Inspection of the tabulated fitted curve from Fig. 4B revealed that the anisotropy remains with 7% accuracy constant for all times $t > 25$ ns. From Eq. (4) we have estimated that setting of the t_1 limit to 25 ns results in less then 5% systematic deviation of the final value of r', which is expected to be within the experimental uncertainty. Fortunately, modern MCP-PMTs do not suffer from such afterpulsing which allows setting of t_1 to lower value and, as a consequence, to significantly improve the data collection rate. The upper integration limit was set to 50 ns since there is no significant emission from the probe at later times.

Figure 5 shows dependence of r_∞ on the temperature during the phase transition of the DMPC membranes. We have tested possibility to detect influence of the diffusion membrane potential on the lipid order during the main phase transition. The phase transition was induced by temperature decrease from 35°C to 15°C and then its increase back to 30°C. Temperature was changed with the rate of 2°C/min and about 100 anisotropy readings was measured during the full temperature cycle. Closed circles in Fig. 5 represent the phase transition of liposomes without the membrane potential, i.e. with the aqueous environment identical inside and outside the LUVs. The phase transition temperature t_m was found to be close to 23.5°C, which is consistent with the literature data [35]. By a visual inspection it is seen that the presence of the transmembrane electric field increases the t_m about 1.5°C–2°C. The result is similar to the finding of Antonov [36] who reported similar increase of the t_m in the electric field. The increase was assessed from the electric conductivity of DPPC and

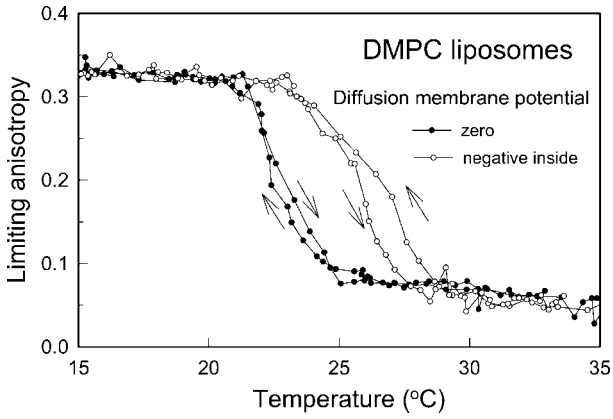

Fig. 5. Temperature dependence of the limiting fluorescence anisotropy r_∞ of DPH in membranes of the DMPC vesicles. Closed and opened circles represent LUVs without and with negative membrane potential, respectively. Arrows indicate heating and cooling of the LUV suspension.

DSPC bilayers. In order to verify that the observed difference is not caused by the presence of choline ions, instead of K^+, outside the vesicles, the same experiment was performed with LUVs prepared in the TC buffer. Such LUVs had a zero diffusion potential on the membrane. No effect of choline ions on the t_m has been found and the curves for LUVs prepared in the TK and TC buffers within the experimental uncertainty overlapped (data not shown).

It is not ambition of this paper to explain detailed mechanisms how transmembrane potential influences the membrane order. This will be the subject of a separate paper. We rather want to demonstrate a capability of the method and present a proof-of-the-principle experiment. To the best of our knowledge, we are the first who present fluorescent measurements of potential-induced changes of lipid order during the phase transition.

DISCUSSION

We are aware that the presented implementation of the method for measurement of r_∞ has a limitation. We used the TCSPC approach since at present we do not have an access to the gated detection. The limitation is the inherently restricted data acquisition rate. The correct function of the TCSPC requires the data collection rate to be less then about 1% of the excitation repetition frequency in order to avoid systematic errors due to the pileup effect [13]. This certainly influences performance of the method, especially for bright samples.

The gated detection does not suffer by this limitation. Moreover, the initial blast of light which could saturate the detector is gated off together with the scattered excitation. One can work therefore with much brighter samples than it would be possible with a standard detector and measurements of r_∞ can be done much faster. Risetime of the standard side-on PMTs is usually in the range of 1–5 ns, which is sufficient for this application. The response of modern MCP PMTs is even much faster, usually in the subnanosecond time range.

In the last decade there has been increased interest in the time resolved imaging techniques [37]. Number of them use gated PMTs or gated image intensifiers. Recent gated intensifiers can operate at high repetition frequencies with gating pulses as narrow as several hundreds of picoseconds [38–40]. Shutter ratios as high as 10^9–10^{12} has been reported [41]. It is not difficult to imagine implementation of the presented method for the r_∞-imaging where the output is a map of the limiting anisotropy r_∞ or the second-rank order parameter $\langle P_2 \rangle$ in the biological sample.

ACKNOWLEDGMENTS

This work was supported by grants 171/2003 and 175/2002 of the Grant Agency of the Charles University and grant MSM 113200001 of the Ministry of Education, Youth and Sports of the Czech Republic.

REFERENCES

1. D. Toptygin and L. Brand (1995). Determination of DPH order in unoriented vesicles. *J. Fluoresc.* **5**(1), 39–50.
2. P. Wahl (1975). Fluorescence anisotropy of chromophores rotating between two reflecting barriers. *Chem. Phys.* **7**, 210–219.
3. K. J. Kinosita, S. Kawato, and A. Ikegami (1977). A theory of fluorescence polarization decay in membranes. *Biophys. J.* **20**, 289–305.
4. J. R. Lakowicz, F. G. Prendergast, and D. Hogen (1979). Differential polarized phase fluorometric investigations of diphenylhexatriene in lipid bilayers: Quantitation of hindered polarizing rotations. *Biochemistry* **18**, 508–519.
5. S. Kawato, K. Kinosita Jr., and A. Ikegami (1977). Dynamic structure of lipid bilayers studied by nanosecond fluorescence techniques. *Biochemistry* **16**, 2319–2324.
6. L. A. Chen, R. E. Dale, S. Roth, and L. Brand (1977). Nanosecond time-dependent fluorescence depolarization of diphenylhexatriene in dimyristoyllecithin vesicles and determination of "microviscosity". *J. Biol. Chem.* **252**, 2163–2169.
7. R. E. Dale, L. A. Chen, and L. Brand (1977). Rotational relaxation of the "microviscosity" probe diphenylhexatriene in paraffin oil and egg lecithin vesicles. *J. Biol. Chem.* **252**, 7500–7510.
8. F. Jähnig (1979). Structural order of lipids and proteins in membranes: Evaluation of fluorescence anisotropy data. *Proc. Nat. Acad. Sci. U.S.A.* **76**(12), 6361–6365.
9. G. Lipari and A. Szabo (1980). Effect of librational motion on fluorescence depolarization and nuclear magnetic-resonance relaxation in macromolecules and membranes. *Biophys. J.* **30**(3), 489–506.
10. C. Zannoni (1981). A theory of fluorescence depolarization in membranes. *Mol. Phys.* **42**(6), 1303–1320.
11. C. Zannoni, A. Arcioni, and P. Cavatorta (1983). Fluorescence depolarization in liquid-crystals and membrane bilayers. *Chem. Phys. Lipids* **32**(3–4), 179–250.

12. M. P. Heyn (1979). Determination of lipid order parameters rotational correlation times from fluorescence depolartization experiments. *FEBS Lett.* **108**, 359–364.
13. D. V. O'Connor and D. Philips (1984). *Time-Correlated Single Photon Counting*, Academic Press, London.
14. J. R. Lakowicz and B. P. Maliwal (1985). Construction and performance of a variable-frequency phase-modulation fluorometer. *Biophys. Chem.* **21**, 61–78.
15. E. Gratton and M. Limkeman (1983). A continuously variable frequency cross-correlation phase fluorometer with picosecond resolution. *Biophys. J.* **44**(3), 315–324.
16. M. Ameloot, H. Hendrickx, W. Herreman, H. Pottel, F. v. Cauwelaert, and W. v. d. Meer (1984). Effect of orientational order on the decay of the fluorescence anisotropy in membrane suspensions. *Biophys. J.* **46**, 525–539.
17. E. Gratton, B. A. Feddersen, and M. Vandeven (1990). In J. R. Lakowicz (Ed.), *Time-Resolved Laser Spectroscopy in Biochemistry II*, SPIE, pp. 21–25.
18. J. M. Beechem (1992). In J. R. Lakowicz (Ed.), *Time-Resolved Laser Spectroscopy in Biochemistry III*, SPIE, pp. 676–680.
19. B. A. Degraff and J. N. Demas (1994). Direct measurement of rotational correlation times of luminescent ruthenium(II) molecular probes by differential polarized phase fluorometry. *J. Phys. Chem.* **98**(48), 12478–12480.
20. J. N. Demas and B. A. Degraff (1992). Applications of highly luminescent transition-metal complexes in polymer systems. *Makromol. Chem. Macromol. Symp.* **59**, 35–51.
21. E. Terpetschnig, H. Szmacinski, and J. R. Lakowicz (1997). In J. Abelson, M. Simon, L. Brand, and M. L. Johnson (Eds.), *Methods in Enzymology, Vol. 278*, Academic Press, San Diego, pp. 295–321.
22. X. Q. Guo, F. N. Castellano, L. Li, and J. R. Lakowicz (1998). A long-lifetime Ru(II) metal-ligand complex as a membrane probe. *Biophys. Chem.* **71**(1), 51–62.
23. L. Li, H. Szmacinski, and J. R. Lakowicz (1997). Long-lifetime lipid probe containing a luminescent metal-ligand complex. *Biospectroscopy* **3**(2), 155–159.
24. L. Li, F. N. Castellano, I. Gryczynski, and J. R. Lakowicz (1999). Long-lifetime lipid rhenium metal-ligand complex for probing membrane dynamics on the microsecond timescale. *Chem. Phys. Lipids* **99**(1), 1–9.
25. D. S. Hanselman, R. Withnell, and G. M. Hieftje (1991). Side-on photomultiplier gating system for thomson scattering and laser-excited atomic fluorescence spectroscopy. *Appl. Spectrosc.* **45**(9), 1553–1560.
26. P. Herman, B. P. Maliwal, and J. R. Lakowicz (2002). Real-time background suppression during frequency domain lifetime measurements. *Anal. Biochem.* **309**(1), 19–26.
27. B. G. Barisas and M. D. Leuther (1980). Grid-gated photomultiplier photometer with sub-nanosecond time response. *Rev. Sci. Instrum.* **51**(1), 74–78.
28. J. Vecer, A. A. Kowalczyk, L. Davenport, and R. E. Dale (1993). Reconvolution analysis in time-resolved fluorescence experiments-an alternative approach: Reference-to-excitation-to-fluorescence reconvolution. *Rev. Sci. Instrum.* **64**(12), 3413–3424.
29. W. Van der Meer, H. Pottel, W. Herreman, M. Ameloot, H. Hendrickx, and H. Schroder (1984). Effect of orientational order on the decay of the fluorescence anisotropy in membrane suspensions—A new approximate solution of the rotational diffusion equation. *Biophys. J.* **46**(4), 515–523.
30. P. Herman, I. Konopasek, J. Plasek, and J. Svobodova (1994). Time-resolved polarized fluorescence studies of the temperature adaptation in Bacillus subtilis using DPH and TMA-DPH fluorescent probes. *Biochim. Biophys. Acta* **1190**(1), 1–8.
31. M. J. Hope, M. B. Bally, G. Webb, and P. R. Cullis (1985). Production of large unilamellar vesicles by a rapid extrusion procedure—characterization of size distribution, trapped volume and ability to maintain a membrane-potential. *Biochim. Et Biophys. Acta* **812**(1), 55–65.
32. J. Vecer, P. Herman, and A. Holoubek (1997). Diffusion membrane potential in liposomes: Setting by ion gradients, absolute calibration and monitoring of fast changes by spectral shifts of diS-C-3(3) fluorescence maximum. *Biochim. Biophys. Acta-Biomembr.* **1325**(2), 155–164.
33. D. Gaskova, H. Kurzweilova, B. Denksteinova, P. Herman, J. Vecer, K. Sigler, J. Plasek, and J. Malinsky (1994). Study of membrane potential changes of yeast cells caused by killer toxin K1. *Folia Microbiol.* **39**(6), 523–525.
34. B. Denksteinova, D. Gaskova, P. Herman, J. Malinsky, J. Plasek, K. Sigler, and J. Vecer (1997). Study of membrane potential changes of yeast cells based on the spectroscopic analysis of diS-C-3(3) fluorescence. *Phys. Med.* **13**, 269–271.
35. J. R. Lakowicz (1980). Fluorescence spectroscopic investigations of the dynamic properties of proteins, membranes and nucleic-acids. *J. Biochem. Biophys. Methods* **2**(1–2), 91–119.
36. V. F. Antonov, E. Y. Smirnova, and E. V. Shevchenko (1989). Electric-field raises phase-transition temperature of Blm of phosphatidic-acid. *Biofizika* **34**(4), 584–588.
37. P. Herman, H.-J. Lin, and J. R. Lakowicz (2003). In Vo-Dingh (Ed.), *CRC Biomedical Photonics Handbook*, CRC Press, New York, pp. 1–30.
38. *Image Intensifiers: Hamamatsu Photonics K. K.*, Electron Tube Center, Document TII 001E01, 2000.
39. Kentech Instruments Ltd., *Gated Image Intensifiers—Specifications*, 2001.
40. LaVision GmbH, *ICCD Camera Systems—Specifications*, 2001.
41. K. Ushida, T. Nakayama, T. Nakazawa, K. Hamanoue, T. Nagamura, A. Mugishima, and S. Sakimukai (1989). Implementation of an image intensifier coupled with a linear position-sensitive detector for measurements of absorption and emission-spectra from the nanosecond to millisecond time regime. *Rev. Sci. Instrum.* **60**(4), 617–623.